

**REPORT DOCUMENTATION PAGE**

AFRL-SR-AR-TR-03-

0187

Public reporting burden for this collection of information is estimated to average 1 hour per searching data sources, gathering and maintaining the data needed, and completing and reviewing this burden estimate or any other aspect of this collection of information, including suggestions for reducing this burden to Washington Headquarters Service, Directorate for Information Operations and Reports, Paperwork Reduction Project (0704-0188) Washington DC 20503  
**PLEASE DO NOT RETURN YOUR FORM TO THE ABOVE ADDRESS.**

1. REPORT DATE (DD-MM-YYYY) 11-30-2001	2. REPORT DATE final	3. DATES COVERED: (From - To) 12-01-00 - 11-30-01
4. TITLE AND SUBTITLE  Smart patches for monitoring fatigue crack growth in aircraft structures		5a. CONTRACT NUMBER
6. AUTHOR(S)  Jeong-Beom Ihn and Fu-Kuo Chang		5b. GRANT NUMBER F49620-99-1-0282
7. PERFORMING ORGANIZATION NAME(S) AND ADDRESS(ES) Stanford University 651 Serra Street Stanford, CA 94305		5c. PROGRAM ELEMENT NUMBER
9. SPONSORING/MONITORING AGENCY NAME(S) AND ADDRESS(ES) AFOSR 801 N Randolph St Arlington, VA 22203		5d. PROJECT NUMBER
12. DISTRIBUTION AVAILABILITY STATEMENT UL		5e. TASK NUMBER
13. SUPPLEMENTARY NOTES		5f. WORK UNIT NUMBER
14. ABSTRACT		8. PERFORMING ORGANIZATION REPORT NUMBER
15. SUBJECT TERMS		10. SPONSOR/MONITOR'S ACRONYM(S)  AGENCY REPORT NUMBER

**DISTRIBUTION STATEMENT A**  
 Approved for Public Release  
 Distribution Unlimited

20030602 125

**14. ABSTRACT**  
 A built-in cost-effective diagnostic system for monitoring crack growth in aircraft structures was developed, particularly for riveted fuselage joints and cracked aircraft parts with composite bonded patches. Different smart patch designs for crack growth monitoring at fuselage lap joints and cracked parts with composite bonded patches were developed and integrated with the corresponding aircraft parts. Using the diagnostic software, pre-selected diagnostic signals are propagated from a designated piezoelectric actuator to neighboring sensors. The corresponding sensor signals are recorded and compared with a baseline reference, which was recorded earlier. The signal processing technique and a damage index resulting from an interpretation algorithm were developed and implemented for extracting features related to crack growth conditions at the time of measurement. A fatigue test for multi-riveted aluminum lap joint (936 x 462 mm) with smart patches installed was performed and the damage index results were compared with conventional NDT methods including eddy current and ultrasonic scan. The probability of damage detection (POD) was assessed for the damage index comparing with two conventional NDT methods. Also, an aluminum plate repaired with boron/epoxy patch where smart patches were inserted was tested and the results were compared with the crack growth results by a visible inspection.

16. SECURITY CLASSIFICATION OF:			17. LIMITATION OF ABSTRACT	18. NUMBER OF PAGES	19a. NAME OF RESPONSIBLE PERSON
a. REPORT	b. ABSTRACT	c. THIS PAGE	UL	28	Fu-Kuo Chang
					20b. TELEPHONE NUMBER (include area code) 650-723-3466

ONRRR/SEATTLE  
 AUG 21 2002  
 RECEIVED

JUN 24 2002

**Grant No F49620-99-1-0282**

Period: 6/1/99 to 11/30/01

**SMART PATCHES FOR MONITORING FATIGUE CRACK GROWTH IN AIRCRAFT  
STRUCTURES**

Final Report

Submitted to  
Dr. Dean Mook

Program Manager for Structural Dynamics  
Air Force Office of Scientific Research  
801 N Randolph St  
Arlington, VA 22203

By

Jeong-Beom Ihn and Fu-Kuo Chang  
Dept. of Aeronautics and Astronautics  
Stanford University, Stanford, CA 94305  
Tel: (650) 723-3466, Fax: (650) 725-3377  
Email: [fkchang@leland.stanford.edu](mailto:fkchang@leland.stanford.edu)

## CONTENTS

<b>Abstract</b> .....	2
<b>1. Introduction</b> .....	3
<b>2. Proposed System</b> .....	4
<b>3. Experiment Setup</b> .....	5
3.1 Riveted Lap joints .....	5
3.2 Bonded Repair Patch .....	6
<b>4. Methodology &amp; Signal Interpretation</b> .....	8
<b>5. Verifying Damage Index</b> .....	14
<b>6. Results</b> .....	16
6.1 Riveted Lap joints .....	16
6.2 Bonded Repair Patch .....	22
<b>7. Conclusions</b> .....	26
<b>8. On-going Research</b> .....	27
<b>9. Acknowledgement</b> .....	27
<b>10. References</b> .....	27

## ABSTRACT

A built-in cost-effective diagnostic system for monitoring crack growth in aircraft structures was developed, particularly for riveted fuselage joints and cracked aircraft parts with composite bonded patches. Different smart patch designs for crack growth monitoring at fuselage lap joints and cracked parts with composite bonded patches were developed and integrated with the corresponding aircraft parts.

Using the diagnostic software, pre-selected diagnostic signals are propagated from a designated piezoelectric actuator to neighboring sensors. The corresponding sensor signals are recorded and compared with a baseline reference, which was recorded earlier. The signal processing technique and a damage index resulting from an interpretation algorithm were developed and implemented for extracting features related to crack growth conditions at the time of measurement. The damage index was verified by a crack propagation test on a notched aluminum plate which was fatigued under cycling loading.

A fatigue test for multi-riveted aluminum lap joint (936 x 462 mm) with smart patches installed was performed and the damage index results were compared with conventional NDT methods including eddy current and ultrasonic scan. The probability of damage detection (POD) was assessed for the damage index comparing with two conventional NDT methods. Also, an aluminum plate repaired with boron/epoxy patch where smart patches were inserted was tested and the results were compared with the crack growth results by a visible inspection. The crack growth prediction of the damage index on both experiments showed a good agreement with NDT predictions as well as visual inspection results.

## 1. INTRODUCTION

Many airplanes flying now have exceeded their design life and the maintenance of these aging aircraft structures has been a world wide issue. The need for a fast, low cost, reliable monitoring system to ensure the safety and functionality of such structures is increasing and has caught the attention of many researchers in structural health monitoring. Aircraft are likely to develop cracks due to cyclic loads and corrosive service environment. Early detection and monitoring of these cracks are the key elements to preventing catastrophic failure and prolonging the life of aircraft structures. For instance, fatigue cracks can initiate at corroded rivet holes and must be detected and repaired before they lead to catastrophic failure<sup>1</sup>.

Current inspection techniques involve complex, time-consuming procedures, which can be very labor-intensive and expensive. Parts may have to be disassembled and re-assembled for inspection, which can cause significant downtime of aircraft and contributes to a most of the inspection effort. Furthermore, bonded repair has become a more common technique for repairing localized damage such as cracks, especially in military aircraft. Although it gives an efficient method for regaining the integrity of the damaged structures, the long-term durability of the patches is not satisfactorily known. Therefore, it is essential to monitor the integrity of the bonded repair in terms of crack growth underneath the patch which can arise from fatigue loading, impact, improper surface preparation, or environmental exposures. The detrimental effects of the long-term environmental exposures on various repair patch systems were investigated by Butkus<sup>2</sup>. Among other repair materials, boron/epoxy patches have become popular for bonded repairs because of their crack arresting capability while maintaining a low patch profile.

Therefore, a fast, low cost built-in diagnostic system is proposed in this study to monitor crack growth from fastener holes in bolted-bonded lap joints or in metallic plates under a composite repair patch.

## 2. PROPOSED SYSTEM

A built-in diagnostic system for monitoring crack growth is proposed as shown in Fig. 1. *SMART Layer<sup>TM</sup>* by Acellent Technologies<sup>3,4,5</sup> made of an array of embedded piezoelectric elements will be installed on 'hot spots' on aircraft and a portable diagnostic system will be connected to the patch to monitor crack growth whenever it's needed. This system will be run by software consisting of diagnostic signal generation, data acquisition, signal interpretation, and a user interface.

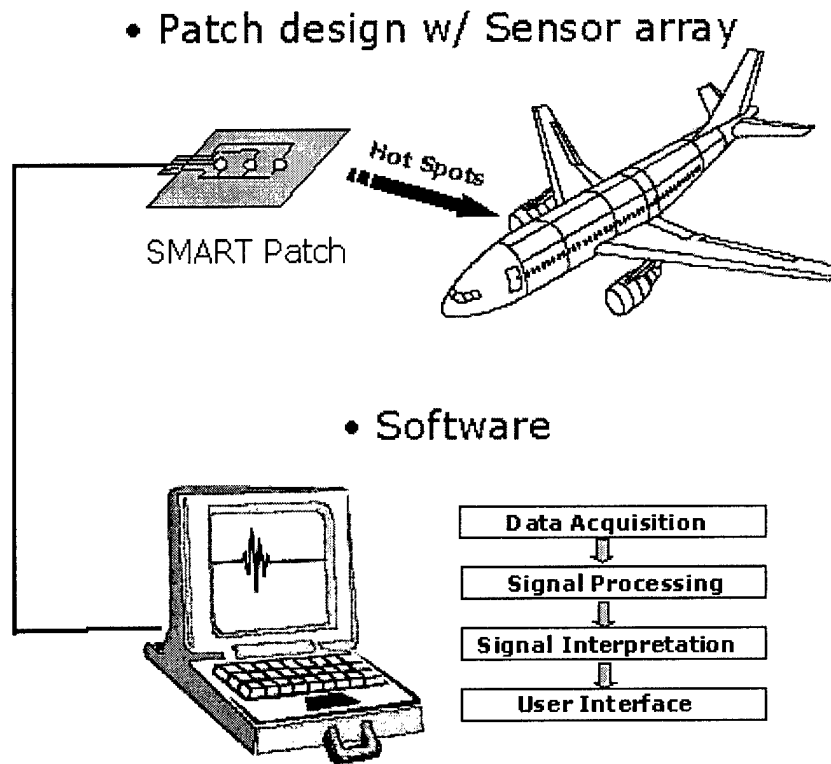


Fig. 1: Built-in diagnostic system

### 3. EXPERIMENT SETUP

#### 3.1 Riveted lap joints

Two identical aluminum single lap joints (936 x 462 mm) with two artificial 1.27 mm edge cracks at the center rivet were used for a constant amplitude fatigue test under tensile loading. Three *SMART Layer<sup>TM</sup>*s by Acellent Technologies were surface mounted as shown in Fig. 2. The center strip located between the two rivet rows was used as an actuator strip and the top and bottom strips were used as sensor strips. Between specified cycle loading intervals, ultrasonic scans and eddy current tests were performed in order to detect crack initiation and growth around 21 rivet holes. No visual inspection was possible on the lap joints.

In parallel with nondestructive testing evaluations, a SMART Suitcase<sup>4</sup> (a portable active diagnostic instrument designed to interface with piezoelectric transducers) was implemented to generate diagnostic signals from the actuator strip and record measurements from the sensor strips. Using a built-in waveform generator, a windowed sine burst wave was generated as an input signal over a wide frequency range 100 ~ 900 kHz and corresponding sensor measurements were collected at a sampling rate of 25 Msample/sec. Processing time for signal generations and sensor data storage took 22 seconds to cover 19 rivets, which is much faster than conventional NDT methods. This processing time is based on the current specification of SMART suitcase by Acellent Technologies<sup>5</sup> and test setups such as sampling points, number of averaging points, frequency bandwidth and etc. Considering only one frequency excitation which likely gives enough information for damage diagnostics, the entire processing time, including interpretation processing time, can be reduced even further.

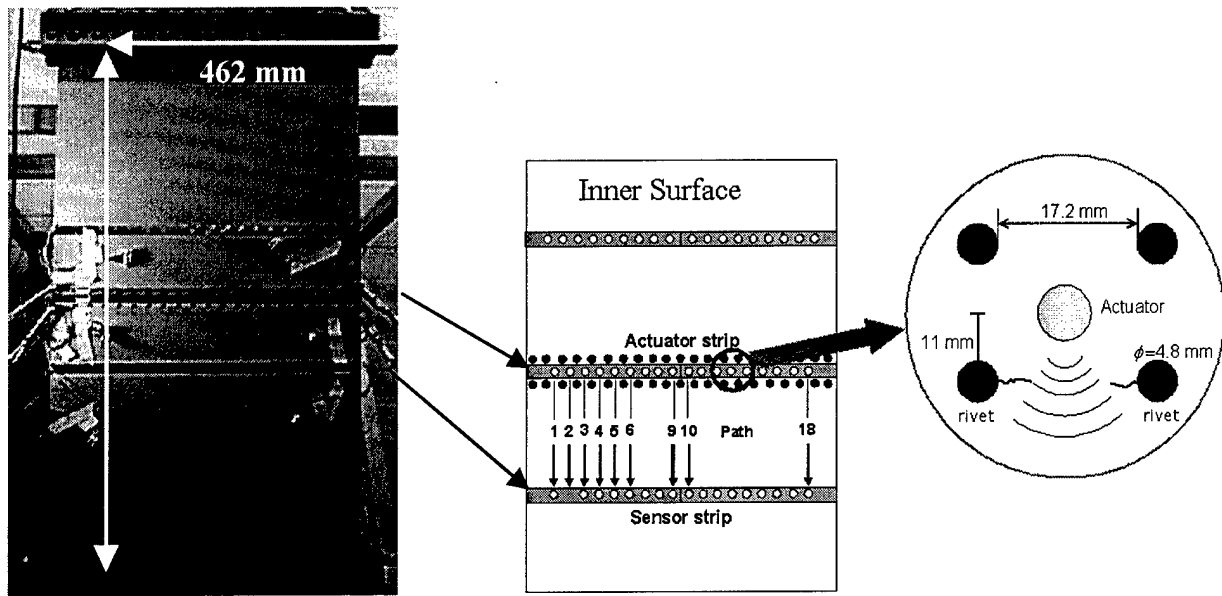


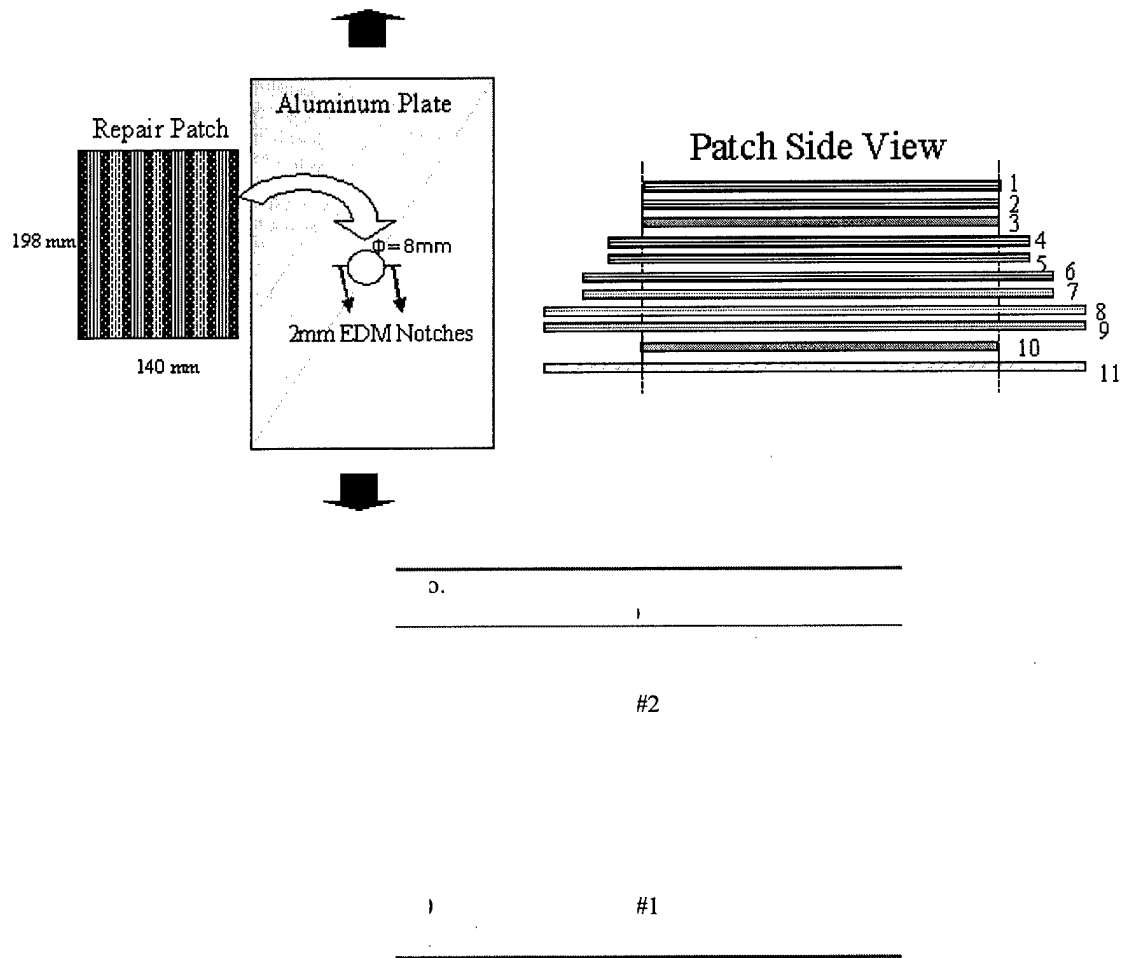
Fig. 2: Lap joint specimen with SMART strips and diagnostic paths

### 3.2 Bonded repair patch

Two rectangular aluminum plates with 2 mm long EDM (Electric Discharge Machining) notches at a center hole (8mm diameter) was repaired with a unidirectional boron/epoxy patch as shown in Fig. 3.

The repair materials used in these tests are listed in Table 1. Two *SMART Layer<sup>TM</sup>*s were fabricated with an embedded network of piezoelectric actuators/sensors and inserted into the patch at different ply location (Fig. 3). The repaired specimen was fatigued by tensile cyclic loading and crack propagation was visually identified from the back side of the repaired panel.

Two specimens were tested with different geometries: one specimen (SMART patch1) has a 140 x 350 mm aluminum base with a tapered patch design and the other (SMART Patch2) has a 420 x 478 mm aluminum base with the same patch design but without the tapered edge. (Fig. 4). The lower *SMART Layer<sup>TM</sup>* (layer 10, Fig. 3) was used for monitoring crack growth in this study. Using a SMART suitcase, an input signal was generated over a frequency range of 100 ~ 600 kHz and sensor measurements were collected after different loading cycles while the specimen was unloaded. The corresponding crack lengths were visually measured.



\* lengths of all layers in SMART Patch2 specimen are 150 mm

Fig. 3: Bonded patch specimen assembly

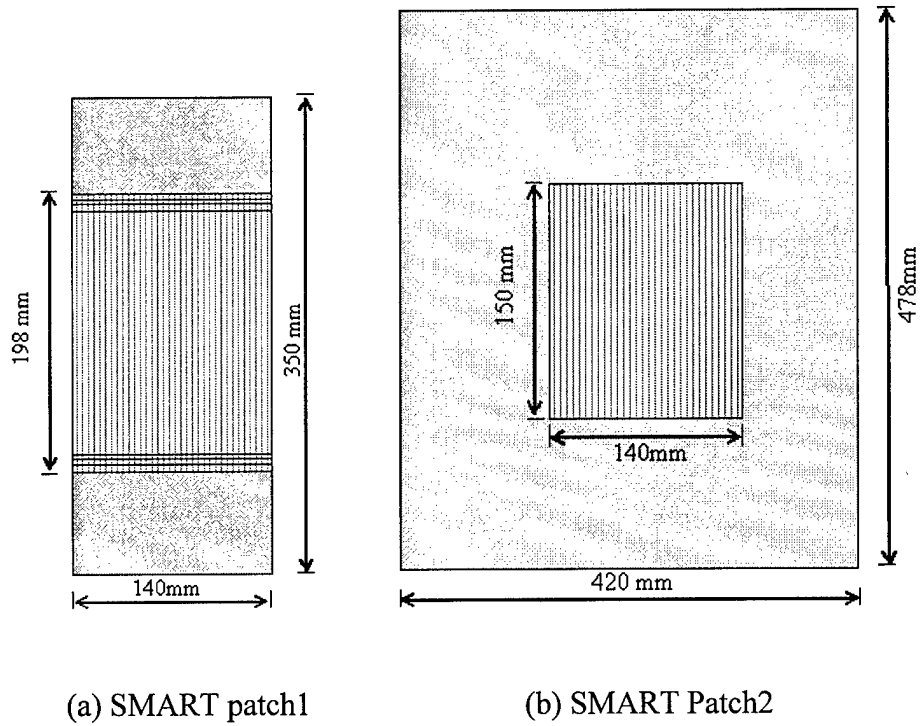


Fig. 4: Bonded patch specimens

ε <sub>preg</sub>
-------------------

Table 1: Bonded patch specimen repair materials

#### 4. METODOLOGY & SIGNAL INTERPRETAION

Lamb waves have been adopted extensively as an effective tool for evaluating defects by detecting changes in the received waveforms. A built-in diagnostic technique was proposed by Roh and Chang<sup>6</sup> to identify an anomaly such as a hole in plates using scattering waves. The interaction of Lamb waves with defects on plates was investigated by Alleyne and Cawley<sup>7</sup>, and the results

showed that the sensitivity of individual Lamb waves to defects was strongly dependent on the frequency. Scattering Lamb waves from a single rivet hole with artificial edge cracks were studied theoretically and numerically by Chang and Mal<sup>8</sup>.

A SMART Suitcase<sup>4</sup> was instrumented to generate diagnostic signals from built in actuators and record measurements at sensors. A five-peak windowed sine burst signal was chosen for the actuator signal and generated over a wide range of frequencies for detecting cracks. When an elastic wave travels through a region where there is a change in material properties, scattering occurs in all directions. The directly transmitted signals are modified to the forward scattering waves, and the scattered energy provides good information about a crack propagating across the actuator and sensor path. The scatter wave in the time domain can be obtained by subtracting the baseline data recorded for the structure with initial damage size from the sensor data for the structure with extended damage size. This scatter wave is a good candidate for the crack detection parameter since it carries information of both amplitude changes and phase changes from the crack propagation.

A joint time-frequency analysis method based on the short-time Fourier Transform (STFT) can be adopted for generating the envelope of the time varying signal and extracting amplitude and time of flight information from sensor measurements.

The STFT of a signal  $s(t)$  is defined as:

$$S(\omega, t) = \frac{1}{2\pi} \int e^{-i\omega\tau} s(\tau)h(\tau - t)d\tau \quad (1)$$

The plots of spectral amplitude information in time and frequency axes are called spectrograms and the wide-band spectrogram can be constructed from the short-time Fourier Transform processes of the collected data at different center frequencies. As an example, Fig. 5 and Fig. 6 show the collected actuator signals from 100 to 700 kHz and the corresponding actuator spectrogram respectively. The spectrogram of sensor measurements can also show the dispersion relation of Lamb waves in time and frequency axis (Fig. 7). Using the spectrogram of the scattered

wave (called ‘scatter spectrogram’), the time varying power spectral density of the scattered wave at a fixed frequency can be generated (Fig. 11).

An interactive Windows program called ‘Disperse’<sup>10</sup>, for generating dispersion curves for a wide range of composite structures, was developed by Pavlakovic and Lowe and utilized in this study. Using Disperse, a group velocity dispersion curve for an aluminum plate can be generated and various Lamb wave modes can be numerically simulated at different center frequencies. Fig. 9 shows a good match in time domain between experiment result and Disperse simulated result of the s0 mode. Using the STFT-envelope method previously described, the group velocity dispersion curve of an aluminum plate can be plotted for fundamental modes and compared with the numerical results (Fig. 8). As noticed in Fig 7 and Fig 8, the ability to get separate information from two fundamental modes experimentally is limited as the group velocities of two fundamental modes become closer and start to overlap in time domain. In order to fully use our measured signals, a mode decomposition method for separating superimposed waves including boundary reflections was studied by Shi and Ihn<sup>11</sup>.

Using the simulated result for the fundamental symmetric mode (s0), the s0-time-window with the lower and upper bound can be estimated (Fig. 10). Damage index is defined as the time integration of the power scatter spectral density within the s0-time-window at a specified frequency. The damage index can be non-dimensionalized by baseline information such that:

$$\text{Damage index} = \frac{\int_{t_i}^{-t_f} |S_{sc}(\omega_0, t)|^2 dt}{\int_{t_i}^{t_f} |S_b(\omega_0, t)|^2 dt} \sqrt{\frac{1}{2}} \quad (2)$$

where  $S_{sc}$  denotes spectral density of scatter signal,  $S_b$  denotes spectral density of baseline signal,  $\omega_0$  denotes the selected frequency,  $t_f$  and  $t_i$  denote the upper bound and lower bound of the fundamental symmetric mode in time domain respectively.

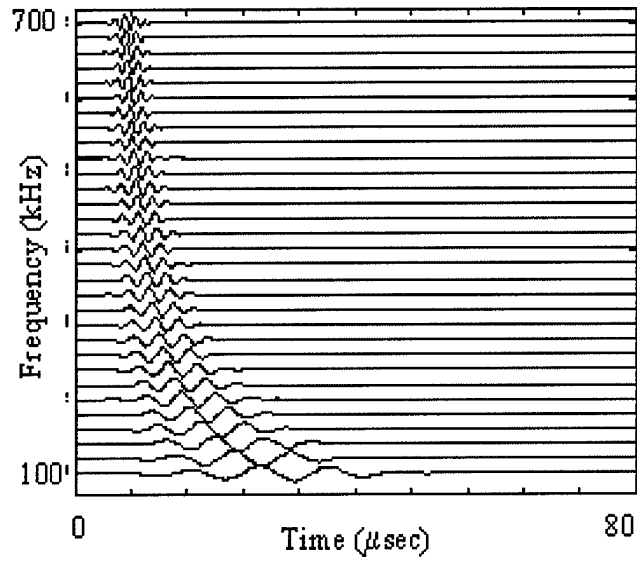


Fig. 5: Collected Multi Frequency Signals

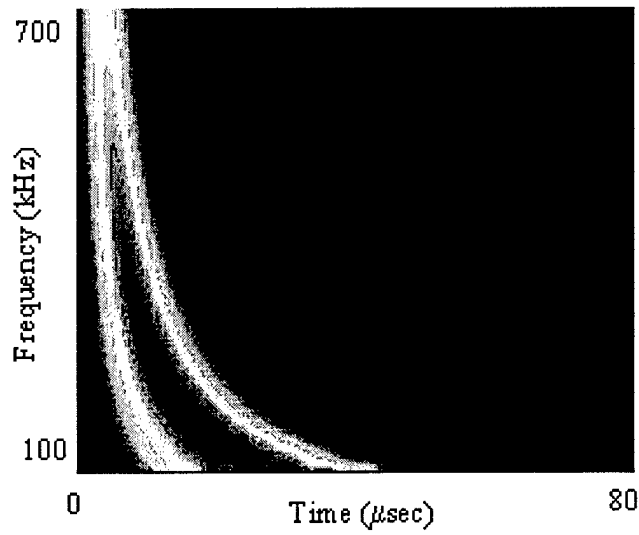


Fig. 6: Actuator Spectrogram

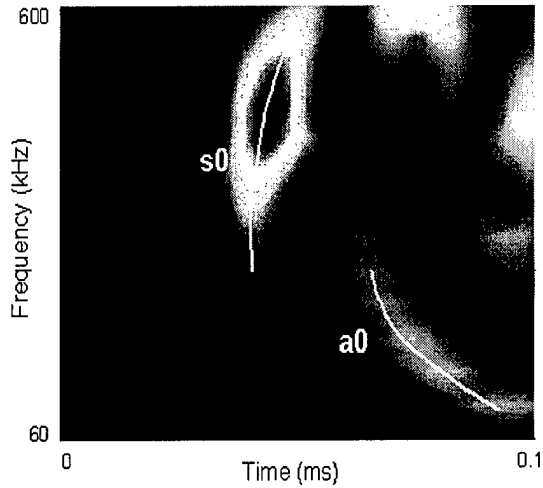


Fig7: Sensor spectrogram

(3.175 mm thick aluminum plate with 180mm actuator-sensor spacing)

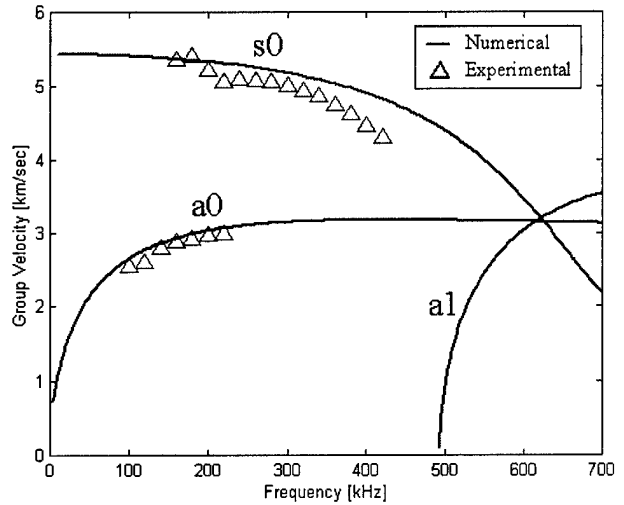


Fig. 8: Group velocity dispersion curve

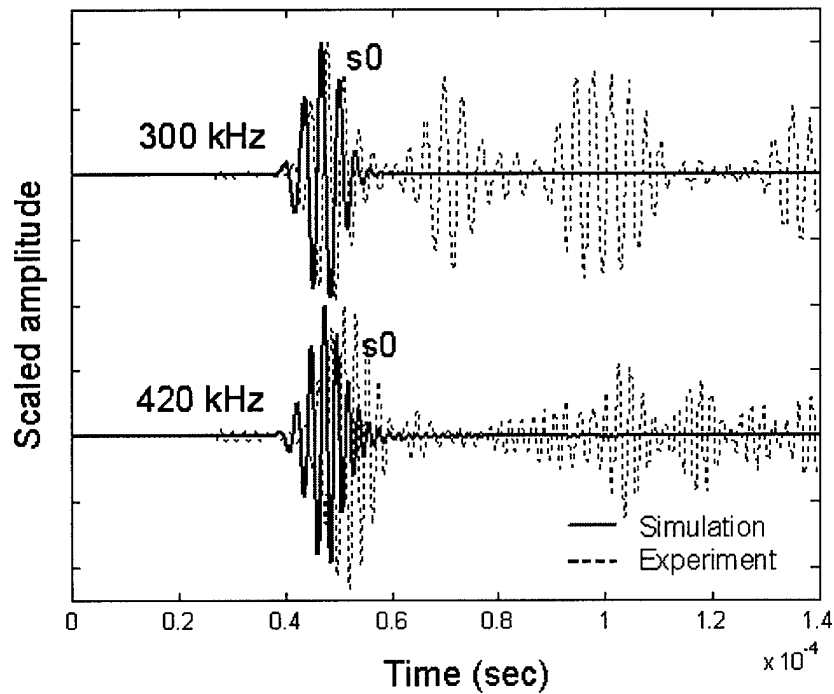


Fig 9: s0 mode comparison

(3.175 mm thick aluminum plate with 180mm actuator-sensor spacing)

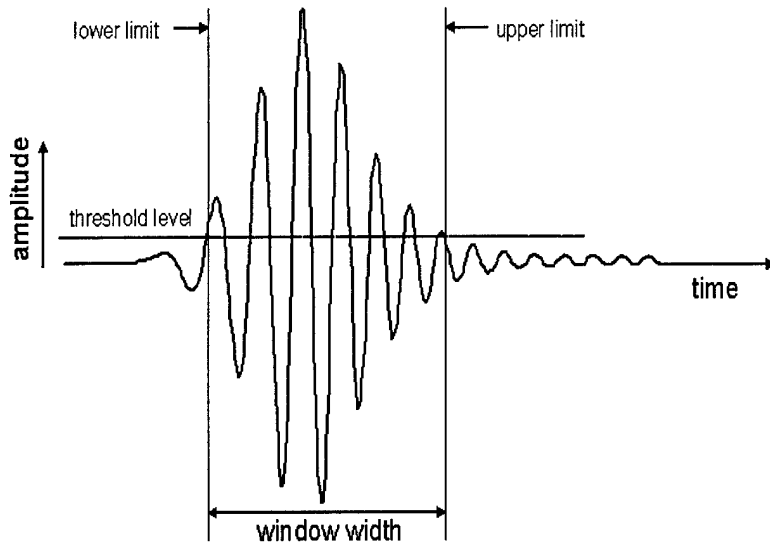


Fig 10: s0-window estimation

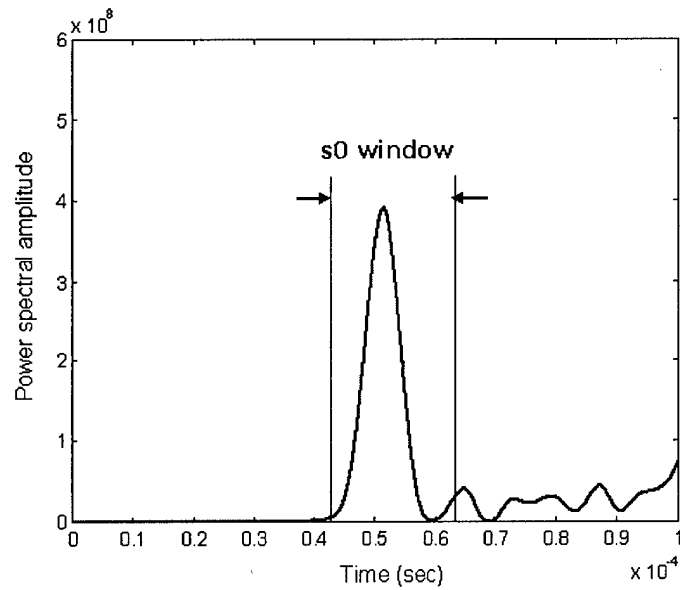


Fig 11: Scatter power spectral density at 420kHz with s0-window

## 5. VERIFYING DAMAGE INDEX

An aluminum plate (300 x 440 x 3.175 mm) with a machined notch (Fig. 12) was fatigued under cyclic loading and crack propagation starting from the notch could be visually observed. At different crack lengths, the load was removed and sensor measurements of surface mounted piezoelectrics were collected from different actuator-sensor paths for a wide range of frequencies (60 ~ 600 kHz).

In Fig. 13, the damage index (DI) was evaluated for path 1 to path3 and plotted against crack growth which is a difference between final crack length and initial crack length ( $a - a_i$ ). The index value of about 0.2, a point where the slope changes, indicates the location of crack tip being at the line of actuator-sensor paths. As a crack tip passes through the paths, the sensitivity (slope) of the DI for all three paths remains the same independent of crack lengths. The sensitivity of the DI to crack growth can be altered by taking different input frequency and baseline data.

Fig 14 shows the DI having almost the same sensitivity for all three paths by choosing baselines with keeping the normal distance from each path to the initial crack tip locations the same (path 1 uses a baseline when  $a_i = 20\text{mm}$ , path 2 when  $a_i = 40$  and path 3 when  $a_i = 70\text{mm}$ ). The damage index approaches to a value of 1 as crack propagates sufficient distance away from the actuator-sensor paths.

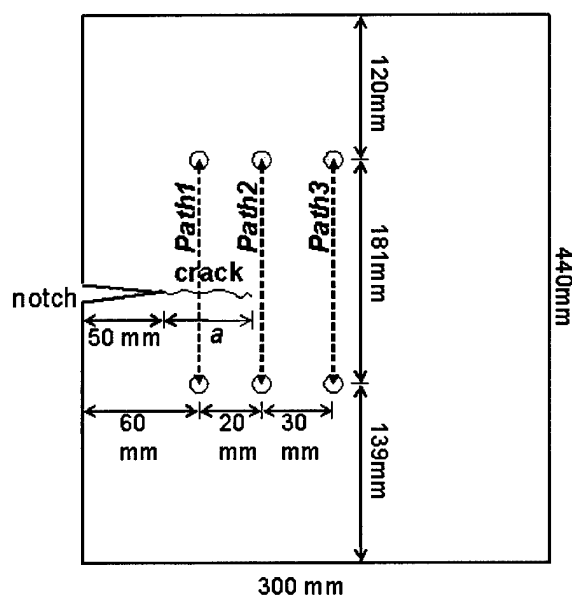


Fig 12: 3.175 mm thick Aluminum plate with a 50 mm machine notch

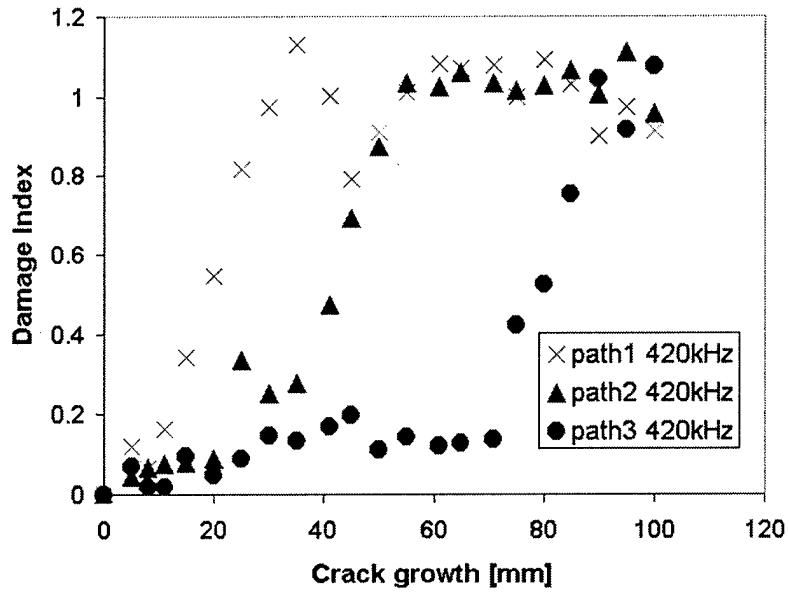


Fig. 13: Damage index vs. crack growth from  $a_i=0$

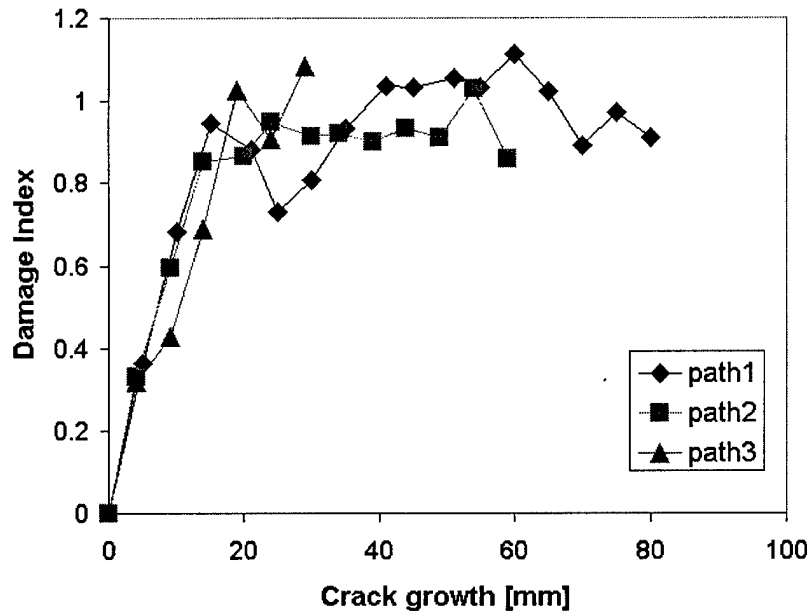


Fig. 14: Damage index vs. crack growth with  $a_i=20$ mm for path 1, 40mm for path 2 and 70mm for path 3

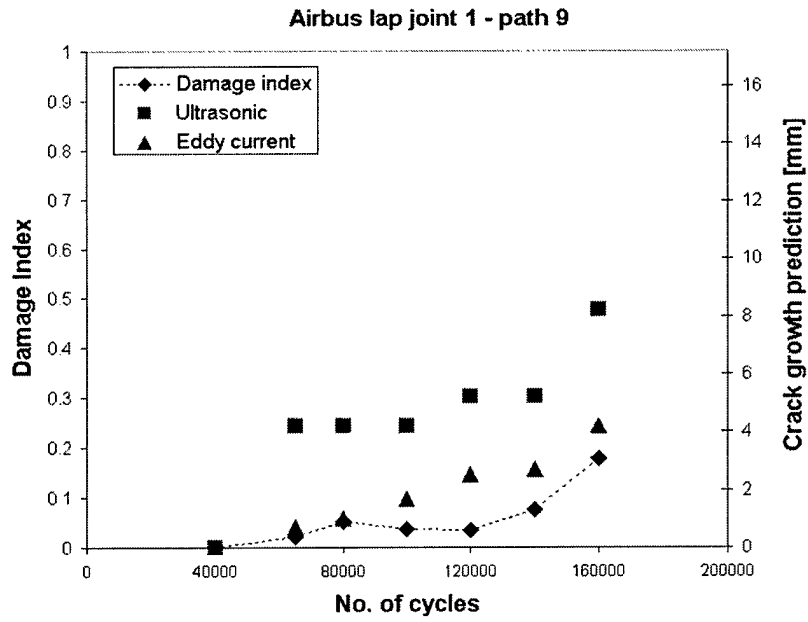
## 6. RESULTS

### 6.1 Riveted Lap joints

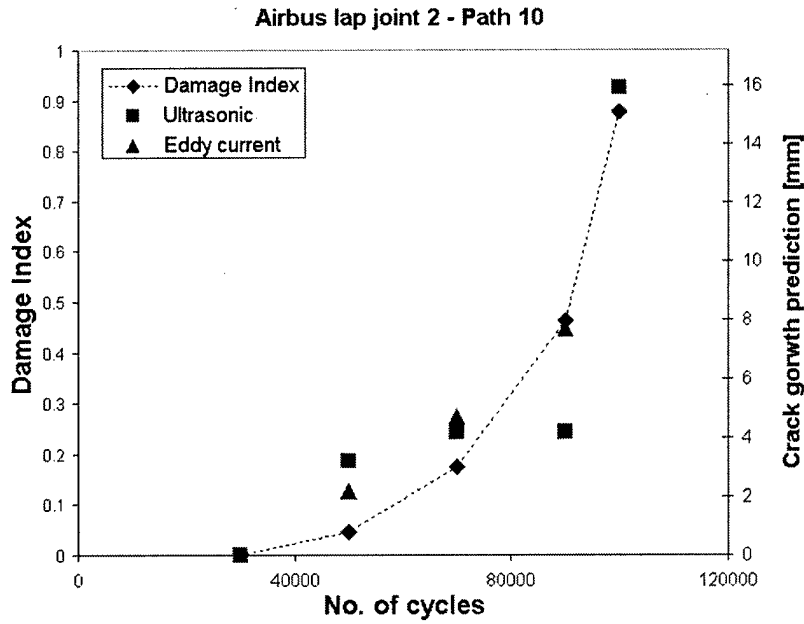
The damage index was evaluated with the sensor measurements from 420 kHz input signals where it gave the highest signal to noise ratio. Between the specified cycle loading intervals, the ultrasonic scan and eddy current test were performed in order to detect crack initiation and growth around 21 rivet holes (Fig. 16 (a),(b)). No visual inspection was possible due to the doublers installed at the joints.

Among the crack estimate results at 18 actuator-sensor paths for each lap joint specimen, Fig. 15 shows the damage index vs. number of cycles along with NDT estimates on the secondary axis at the selected paths. Since different NDT techniques have different crack detection resolution (Fig. 16), the damage index shows different correlation with ultrasonic and eddy current crack estimates in Fig. 17.

POD (probability of detection) is a characteristic how to quantify the quality of any NDT technique. For this the different crack events having been monitored by NDT were ranked from the largest down to the smallest crack length and then compared with the results obtained with the damage index. The procedure of POD analysis is explained in more detail in the previous paper<sup>9</sup>. POD was evaluated in Fig 18, 19, and 20. In Fig. 18 and 19, two threshold levels of the damage index were used for POD and a damage index of 0.1 is a good threshold level where crack lengths down to 5 mm can be detected and still avoids false calls when compared with conventional NDT estimates (Fig. 17). Also, the damage index shows a higher probability of damage detection with eddy current than ultrasonic technique (Fig. 20).



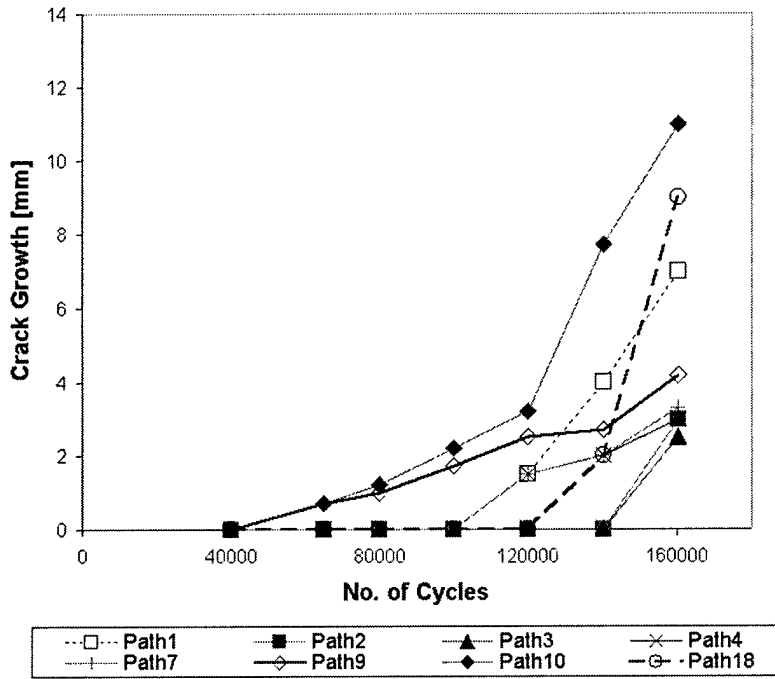
(a)



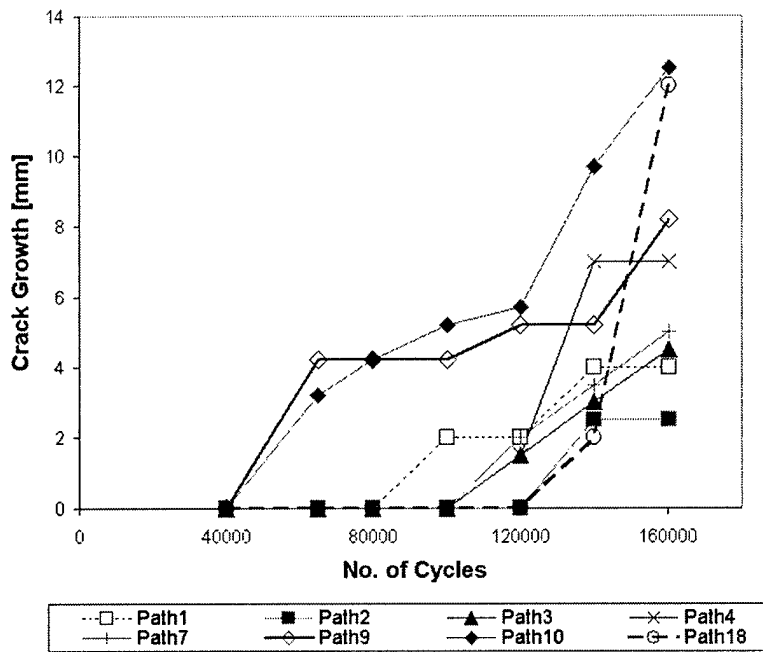
(b)

Fig. 15: Damage Index vs. no. of cycles with NDT estimate in secondary axis

(a) Airbus lap joint 1- path 9; (b) Airbus lap joint 2 - path 10

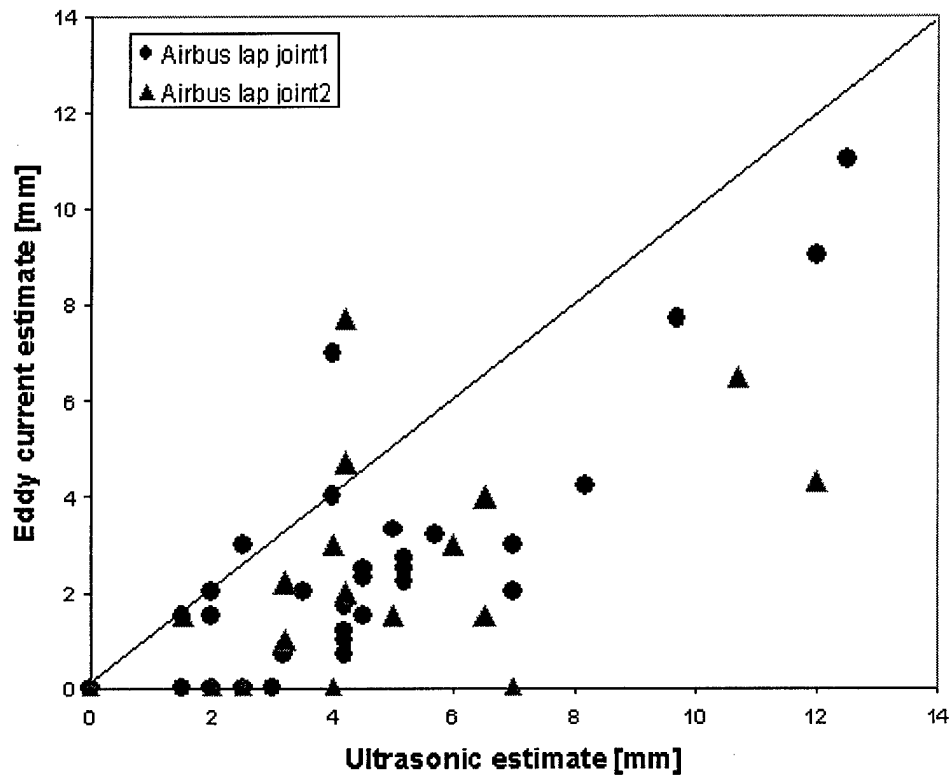


(a) Eddy current crack growth estimate



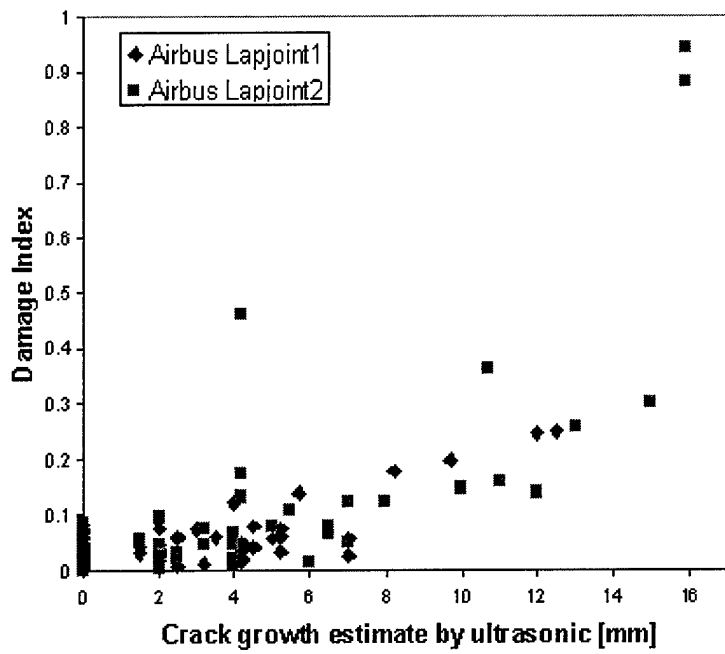
(b) Ultrasonic crack growth estimate

max. estimate difference = 7.7 mm

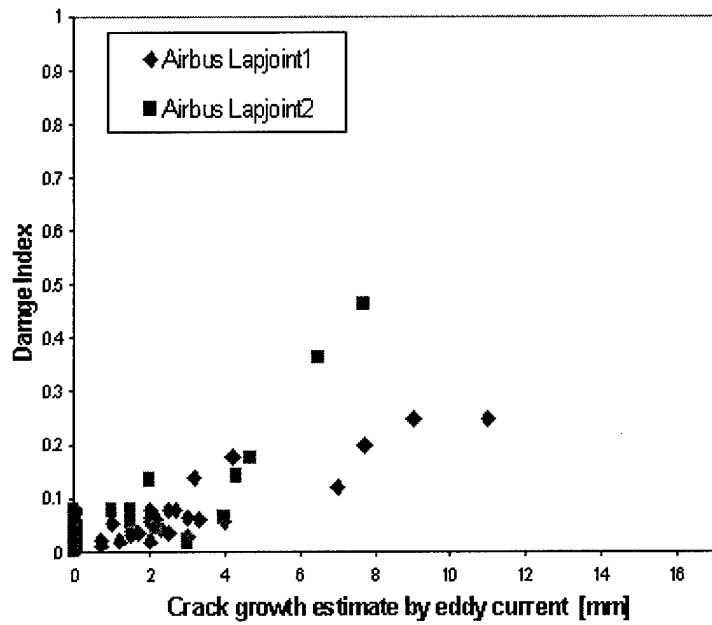


(c) Eddy current vs. ultrasonic

Fig. 16: Comparison of NDT techniques



(a) Damage index vs. eddy current



(b) Damage index vs. ultrasonic

Fig. 17: Damage Index vs. NDT crack growth estimate

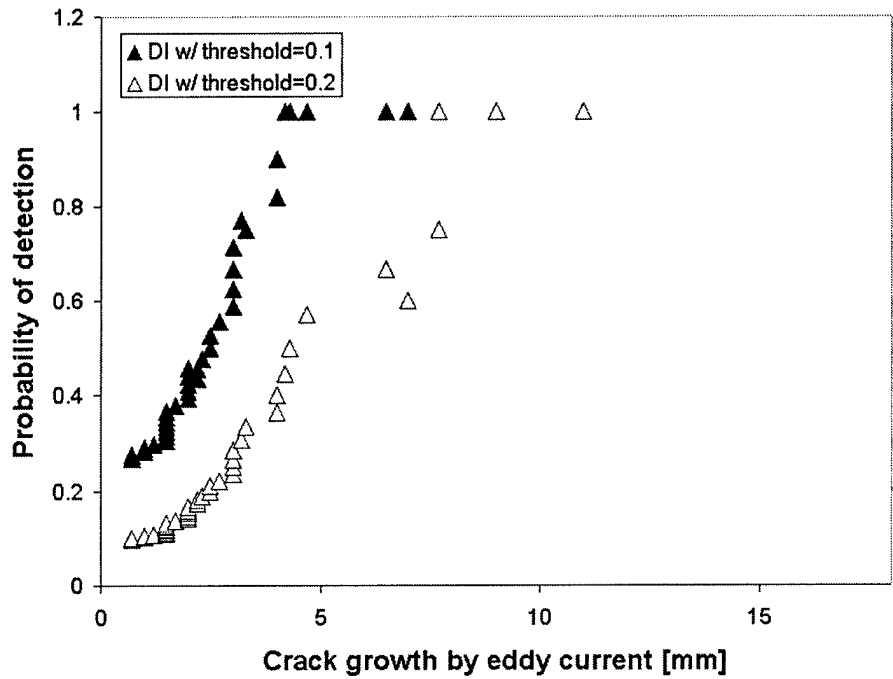


Fig. 18: Probability of damage detection by the damage index when compared to eddy current NDT

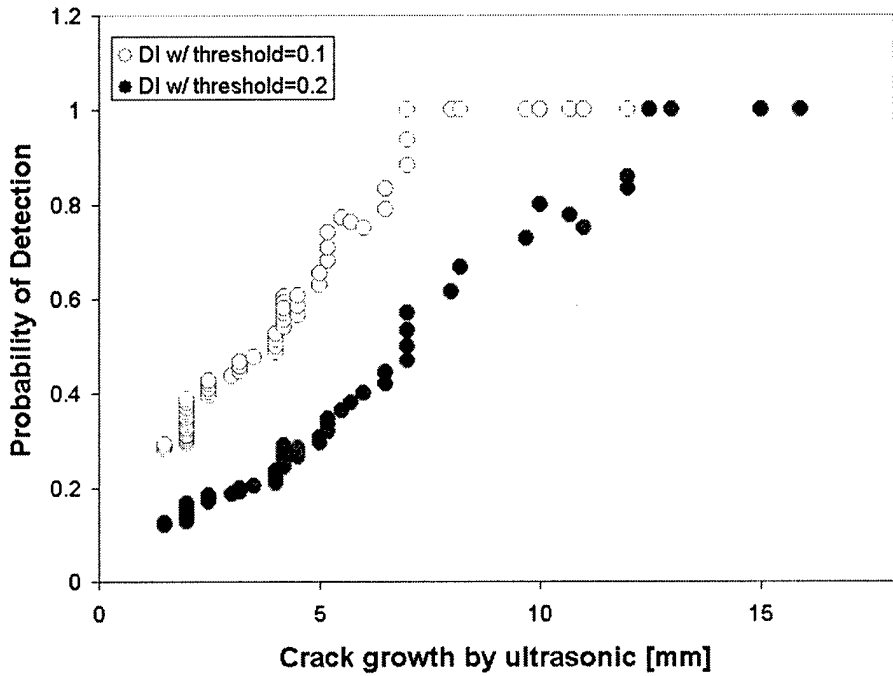


Fig. 19: Probability of damage detection by the damage index when compared to ultrasonic NDT

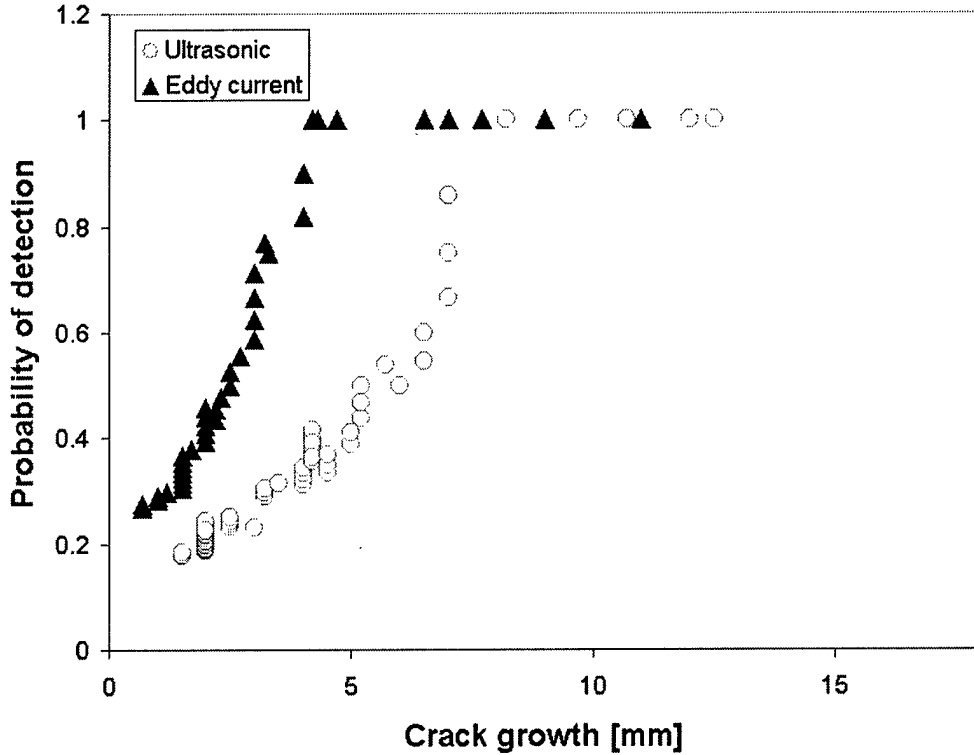


Fig. 20: Probability of damage detection by the damage index when compared to ultrasonic and eddy current NDT

## 6.2 Bonded Repair Patch

The Boron/Epoxy patch-Adhesive Layer-Aluminum plate specimen described earlier was modeled using the Disperse code and the group velocity dispersion curve including various modes was generated (Fig. 21). The stiffness of the boron/epoxy patch was taken as  $C_{11} = 210.1$  GPa,  $C_{12} = C_{13} = 5.64$  GPa,  $C_{22} = C_{33} = 26.3$  GPa,  $C_{23} = 4.5$  GPa, with shear stiffness  $C_{44} = 10.3$  GPa,  $C_{55} = C_{66} = 7.2$  GPa. A Young's modulus of 2.07 GPa and a Poisson's ratio of 0.34 were used for the adhesive layer. Based on the group velocity plot of fundamental Lamb wave modes, the wave packet of fundamental symmetric mode (s0) was identified from its group velocity measurement and used for the analysis. Fig 21 shows a good agreement between numerical results and experimental measurements at frequency range of 380 ~ 460 kHz.

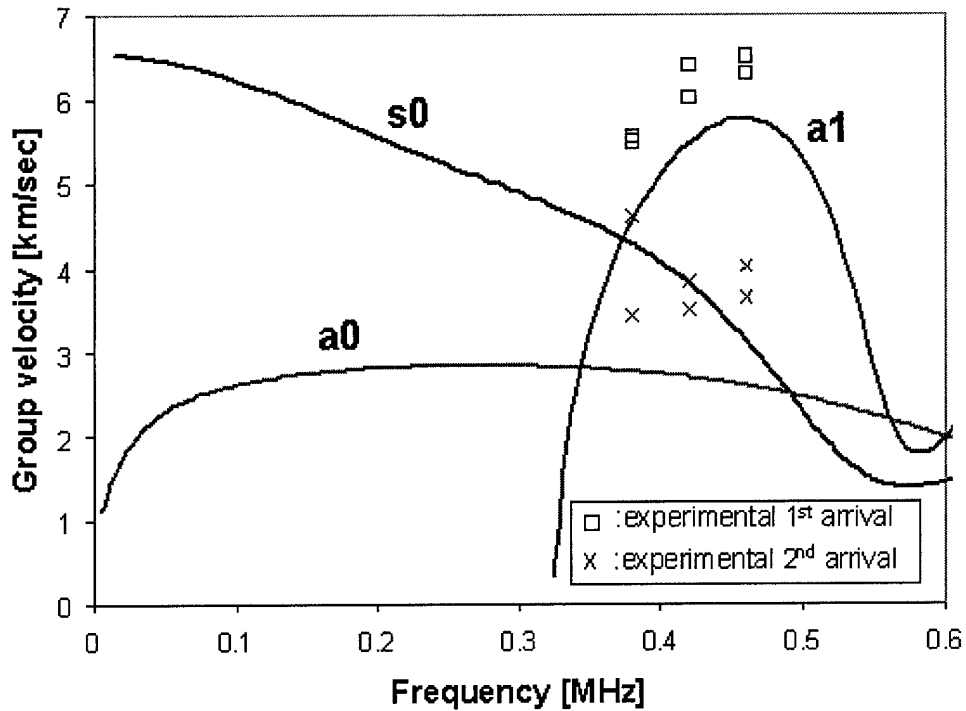


Fig. 21: Group velocity dispersion curve of Boron/Epoxy-Adhesive-Aluminum (fiber direction)

The sensor data from 420 kHz input signal was used for the analysis due to having the highest signal to noise ratio. The damage index was evaluated based on the time arrival of a s0 wave which was verified by the dispersion curve of the born/epoxy-adhesive-aluminum system (Fig. 21). The baseline was taken after the specimens were cycled until an initial crack growth of 2mm had occurred. The further crack growth was visually identified and at the same time monitored by the damage index which was evaluated at different diagnostic paths (Fig. 22). The results are plotted in Fig. 23, which indicates the clear crack growth detection capability of the damage index. It also shows in a consistent manner the higher sensitivity of the damage index as the diagnostic paths (Path B & C) are closer to the initial crack tip location.

In order to evaluate the cyclic loading effect on the damage index, the sensor measurements were continuously taken at the specified loading intervals even before any visual identification of

crack initiation was possible. Fig. 24 shows the changes of the damage index at different loading cycles but the variation remains at a low value less than 0.1.

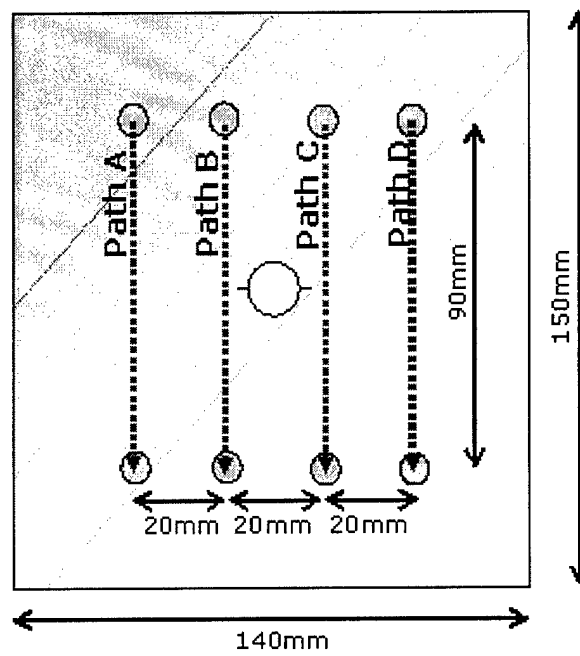
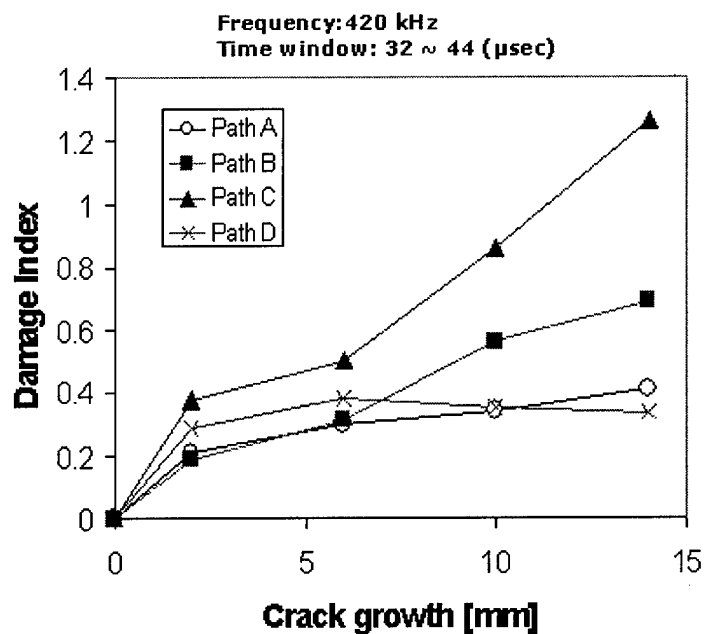
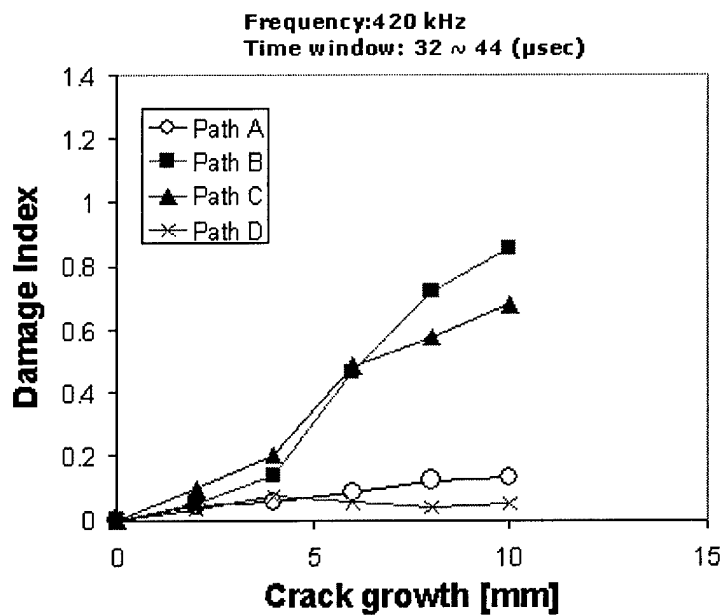


Fig. 22: Diagnostic paths in SMART layer



(a)



(b)

Fig. 23: Damage index vs. crack growth  
(a) SMART Patch1; (b) SMART Patch2;

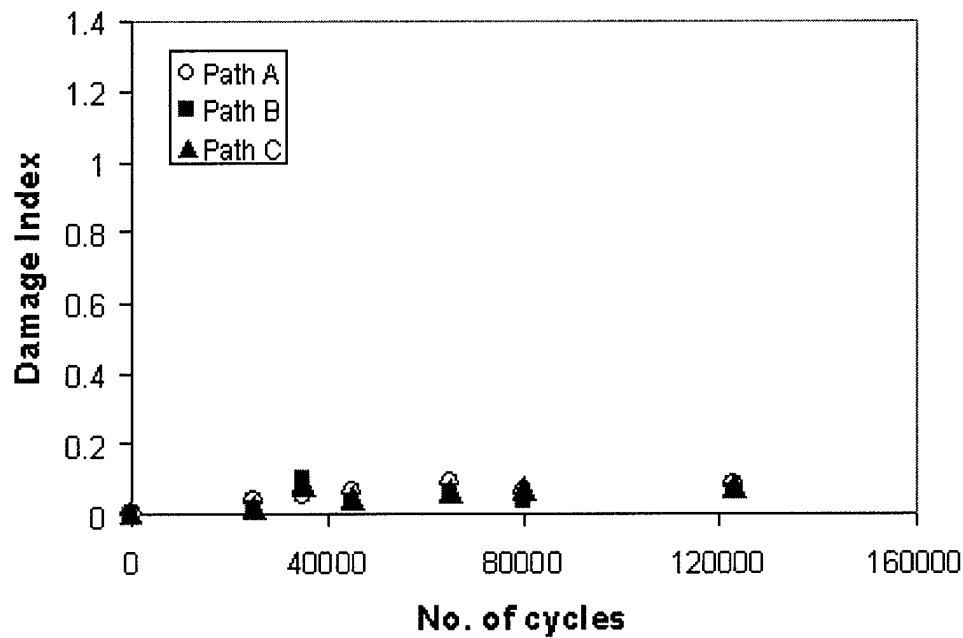


Fig. 24: Cyclic loading effect on the damage index

## 7. CONCLUSIONS

A fast and cost-effective built-in diagnostic system was developed for monitoring crack growth in bolted-bonded lap joints and in a metallic plate under a composite repair patch. The system consists of piezoelectric sensor layers, a portable diagnostic unit, and software. Signal processing and interpretation algorithms (damage index) were developed for the proposed system. In riveted lap joints, the damage index can be potentially used to detect crack lengths as small as 5mm with certainty equal to conventional NDT. Due to the uncertainties involved in NDT estimates, the damage index value cannot be directly related to real crack lengths at this time but it can provide information of 'crack (5mm or longer)' or 'no crack (shorter than 5mm) condition with good confidence. Also, the results from the repair patch specimens clearly indicate that the embedded SMART patch can detect crack propagation underneath the patch using the same damage detection algorithm. Using this crack monitoring system with piezoelectric sensor layers, or SMART patches, which can be easily integrated with aircraft parts such as lap joints or composite repair

patches, inspection effort can be significantly reduced and can be a basis for condition based health monitoring of aircraft.

## 8. ON-GOING RESERACH

The repair patch can be locally delaminated from the host structure due to fatigue loading and harsh service environments. The patch debond effect on damage index and a scheme to monitor the debond area are being developed. The optimal actuator/sensor locations needed for enhancing the detection ability of damage index are being investigated. Please refer to the author's Ph. D. dissertation paper for up-to-date results and information.

## 9. ACKNOWLEDGEMENT

The support of the AFOSR ( No. F49620-99-1-0282) is gratefully acknowledged. Dean Mook is the Program Manager.

## 10. REFERENCES

1. R. Jones, L. Molent, S. Pitt, "Study of multi-site damage of fuselage lap joints", *Theoretical and Applied Fracture Mechanics*, 32, p.81-100, 1999.
2. Lawrence M. Butkus, "Environmental durability of adhesively bonded joints", Ph.D. Dissertation, Department of Mechanical Engineering, Georgia Institute of Technology, 1997.
3. M. Lin, "Manufacturing of Composite Structures with a Built-In Network of Piezoceramics", Ph.D. Dissertation, Department of Mechanical Engineering, Stanford University, Stanford, 1998.

4. M. Lin, X. Qing, A. Kumar, and S. Beard, "SMART Layer and SMART Suitcase for Structural Health Monitoring Applications", *Proceedings of SPIE on Smart Structures and Material Systems*, March 2001.
5. Acellent technologies <http://www.acellent.com>
6. Y.S. Roh, "Built in diagnostics for identifying an anomaly in plates using wave scattering", Ph.D. Dissertation, Department of Aeronautics and Astronautics, Stanford University, 1999.
7. D. N. Alleyne, P. Cawley, "The interaction of Lamb waves with defects", *IEEE Trans. Ultrasonics, Ferroelectrics, and frequency control*, 39, p.381-397, 1992.
8. Z. Chang, A. Mal, "Scattering of Lamb waves from a rivet hole with edge cracks", *Mechanics of Materials*, 21, p.197-204, 1999.
9. C. Boller, J.-B. Ihn, W.J. Staszewski and H. Speckmann, "Design Principles and Inspection Techniques for Long Life Endurance of Aircraft Structures", *Proceedings of the 3rd International Workshop on Structural Health Monitoring*, Stanford, U.S.A., pp.275-283, 2001.
10. B. Pavlakovic and M. Lowe, "A system for generating dispersion curves – user's manual for Disperse v.2.0", June 2000.
11. L. Shi and J. Ihn, "Identification of Time-Domain Reflectometry Measurement Results by Wavelet Modeling", *Proceedings of the 3rd International Workshop on Structural Health Monitoring*, Stanford, U.S.A., pp.1269-1278, 2001.